

# On the Safety of Human Body Communication

Shovan Maity , Mayukh Nath , Gargi Bhattacharya, Baibhab Chatterjee , Student Member, IEEE, and Shreyas Sen , Senior Member, IEEE

Abstract—Human Body Communication (HBC) utilizes the electrical conductivity properties of the human body to communicate between devices in and around the body. The increased energy-efficiency and security provided by HBC compared to traditional radio wave based communication makes it a promising alternative to communicate between energy constrained wearable and implantable devices around the body. However, HBC requires electrical signals to be transmitted through the body, which makes it essential to have a thorough analysis of the safety aspects of such transmission. This paper looks into the compliance of the current density and electric/magnetic fields generated in different modalities of HBC with the established safety standards. Circuit and Finite Element Method (FEM) based simulations are carried out to quantitatively find the compliance of current density and fields with the established safety limits. The results show the currents and fields in capacitive HBC are orders of magnitude smaller than the specified limits. However, certain excitation modalties in galvanic HBC can result in current densities and fields exceeding the safety limits around the excitation point on the body near the electrode. A study with 7 human subjects (4 male, 3 female) is carried out over a month, using capacitive HBC. The study monitors the change in 5 vital parameters (Heart Rate, Mean Arterial Pressure, Respiration Rate, Peripheral Capillary Oxygen Saturation, Temperature), while wearing a HBC enabled device. Analysis of the acquired data statistically shows no significant change in any of the vital parameters of the subjects, confirming the results of the simulation study.

Index Terms—Human body communication (HBC), body coupled communication (BCC), safety standards, capacitive HBC, galvanic HBC.

## I. INTRODUCTION

RAPID scaling in the size and cost of semiconductor technology has resulted in increasing usage of small form factor wearable and implantable devices. These devices communicate with other devices and form a network around the

Manuscript received July 4, 2019; revised December 16, 2019; accepted January 19, 2020. Date of publication April 13, 2020; date of current version November 20, 2020. This work was supported in part by Eli Lilly through the Connected Health care initiative, Air Force Office of Scientific Research YIP Award under Grant FA9550-17-1-0450 and in part by the National Science Foundation CRII Award under Grant CNS 1657455. (Corresponding author: Shreyas Sen.)

Shovan Maity, Mayukh Nath, Gargi Bhattacharya, and Baibhab Chatterjee are with the Department of Electrical and Computer Engineering, Purdue University

Shreyas Sen is with the Department of Electrical and Computer Engineering, Purdue University, West Lafayette, IN 47907 USA (e-mail: shreyas@purdue.edu).

Digital Object Identifier 10.1109/TBME.2020.2986464

human body, known as the Body Area Network (BAN). The traditional method of communication between these devices is through wireless radio wave based protocols such as Bluetooth. Human Body Communication (HBC) [1]–[9], also commonly known as Body Coupled Communication (BCC) [10]-[12] or Intra Body Communication (IBC) [13], is rapidly emerging as an alternative way to communicate between these devices around the human body, which uses the human body as the communication medium. The key advantage provided by HBC over radio wave communication is enhanced energy efficiency and security of communication. The increased energy efficiency can be obtained from utilizing the body as a broadband communication channel [1], [2], [14]. The confinement of the HBC transmitted signal primarily within the human body provides the enhanced physical security which is not present in wireless radio communication, where the signal is isotropically radiated and can be intercepted by any device within a certain range. Both energy-efficiency and security are vital restrictions for small form factor wearable/implantable devices with limited battery life, making HBC even more relevant for such energy and resource constrained [15], [16] devices. This has led to increasing focus on the design of HBC systems both at the circuit [10], [11], [17]-[19] and system [14], [20] level. Recent research [2] has shown that HBC transmission can achieve energy efficiency up to 6.3 pJ/bit making it 100X energy efficient compared to Wireless Body Area Network (WBAN) protocols such as Bluetooth. The enhanced security property of HBC has also been shown in [21] showing signal confinement within 10 cms of the body.

HBC involves transmitting electrical signals through the human body. Hence, the safety aspect of HBC needs to be studied before its widespread adoption. Although there has been multiple safety standards defined on the exposure of human body to time varying electric/magnetic fields and electrical current, there has been surprisingly few studies about the safety aspect of HBC. Most studies, which look into the adverse effect of electricity on the human body, generally deal with much higher voltage and current levels. [22] looks into the different types of interaction between human and computers that require electrical signal transmission through the body and analyzes the safety aspect of some of those studies in terms of the amount of current being injected into the body. In this paper we investigate the safety aspect of HBC through theoretical analysis and experimental validation. The theoretical analysis of compliance of the current and field densities are carried out through circuit and Finite Element Method (FEM) simulations respectively. These simulations provide a quantitative measure of the safety

0018-9294 © 2020 IEEE. Personal use is permitted, but republication/redistribution requires IEEE permission. See https://www.ieee.org/publications/rights/index.html for more information.

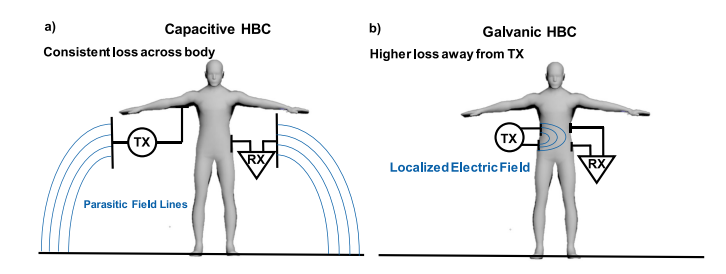


Fig. 1. Different type of HBC: (a) Capacitive HBC with single ended excitation and termination, (b) Galvanic HBC with differential excitation and termination.

compliance of the HBC. Furthermore, studies are carried out to show the effect of HBC on the vitals of human subjects. The simulation results show that the current densities and electric, magnetic field densities induced in HBC are orders of magnitude smaller than the safety standards. A study is carried out on a small set of volunteers to experimentally corroborate the safety margins obtained from the simulations. It is observed that the subjects do not show any significant change in vital parameters while wearing a HBC device, compared to a normal scenario. To the best of the authors' knowledge, this is the first study which provides a comparison of the generated fields and current densities within the body with the safety limits provided by the different standards.

The rest of the paper is organized as follows: Section II discusses the fundamentals of capacitive and galvanic HBC. Section III discusses the different safety standards that is in place for HBC. Section IV does a detailed analysis of the safety compliance of different type of HBC in terms of current density (circuit simulations) and field intensities (FEM simulations). Section V provides an experimental study of the effect of HBC on the vital parameters of subjects. Section VI discusses possible circuit design techniques to ensure HBC safety with conclusion in Section VII.

## II. HUMAN BODY COMMUNICATION: BASICS

HBC utilizes the electrical conductivity property of the human body to send electrical signals through it and use it as a communication medium. The signal is coupled into the body through metal electrode(s). The signal goes through the relatively high impedance skin layer and is primarily transmitted through the low impedance conductive layers underneath the skin [1], [19]. At the receiver end also the signal is picked up through a single electrode/ a pair of electrodes. Depending on the excitation and termination modality, HBC can be primarily divided into two categories: a) Capacitive HBC, b) Galvanic HBC.

#### A. Capacitive HBC

Capacitive HBC was first proposed by Zimmerman [23] as a method of communication between devices on a Personal Area Network (Fig. 1a). The excitation is applied through a single electrode at the transmitter end. The human body provides only the forward path of communication between the transmitter and receiver. However, it is necessary to have a closed loop

path between the transmitter and receiver to enable electrical communication. In case of capacitive HBC, the closed loop is formed through capacitances formed by parasitic coupling of the transmitter/receiver ground with the surrounding environment, which acts as the earth ground. The channel loss between the transmitter and receiver is strongly dependent on this return path capacitance. As a result, in capacitive HBC, the channel loss is strongly dependent on the surrounding environment of the person. However, the loss is almost independent of the distance between the devices on the body [1]. This makes capacitive HBC the primary choice for long distance communication on the body (between two arms, arm to torso etc.)

#### B. Galvanic HBC

Wegmueller et al. [24] proposed galvanic HBC as an alternative to capacitive HBC (Fig. 1b). In galvanic HBC, the signal is applied to the body through a pair of electrodes in a differential manner. The reception is also done in a differential manner at the receiver end. Hence, the closed loop path between the transmitter and receiver is formed through the human body in this scenario. This makes galvanic HBC more robust to environmental variation, as the channel loss is completely dependent on the human body parameters and not on the surrounding environmental factors. Since the transmitter forms a closed loop through the body in this scenario, most of the electric field is contained directly between the signal and ground electrode at the transmitter end. A small fraction of the fringing electric field between the transmitter electrodes actually reach the receiver end for it to sense as a voltage differentially. The fraction of field reaching the receiver reduces as the distance between the transmitter and receiver increases. Consequently, the channel loss increases as the distance between the transmitter and receiver increase. This makes the channel loss dependent on the distance between the transmitter and receiver in galvanic HBC [25]. Galvanic HBC is particularly useful for short distance communication between wearable devices (between an arm and wrist worn device) but not suitable for HBC between wearable devices with longer channel

In the subsequent sections we discuss about the safety standards and look into the safety margins of the two different type of HBC.

## III. SAFETY LIMITS OF HUMAN BODY COMMUNICATION

There are multiple standards specifying the safety limits on the exposure of human body to electric/magnetic fields. We look into the safety limits provided by three primary safety standards in this section.

# A. International Commission on Non-Ionizing Radiation Protection (ICNIRP) Standard

In HBC systems, the impact of signal transmission through human body and its safety limits must be carefully addressed. The International Commission on Non-Ionizing Radiation Protection (ICNIRP) [26] provides the exposure limit of Non Ionizing Radiation for humans. Depending on the frequency of the

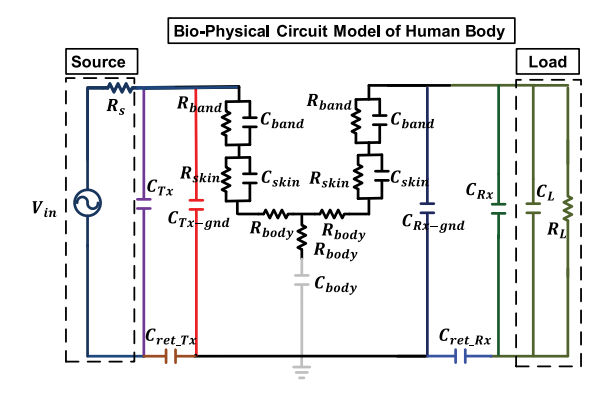


Fig. 2. Detailed Bio-physical model of HBC [1] showing the different biological parameters and load conditions. The different parameters are as follows:  $R_s$ : Source Resistance,  $C_{Tx}$ : Transmitter ground to body capacitance,  $C_{Tx-gnd}$ : Capacitance between body and ground at the transmitter end,  $C_{ret\_Tx}$ : Return path capacitance of the transmitter,  $R_{band}$ : Resistance of the coupling electrode,  $C_{band}$ : Capacitance of the coupling electrode,  $R_{skin}$ : Skin resistance,  $C_{skin}$ : Skin capacitance,  $R_{body}$ : Tissue resistance,  $C_{body}$ : Capacitance between feet and ground,  $C_{Rx-gnd}$ : Capacitance between body and ground at the receiver end,  $C_{ret\_Rx}$ : Return path capacitance of the receiver,  $C_{Rx}$ : Receiver ground to body capacitance,  $C_L$ : Load capacitance,  $R_L$ : Load resistance.

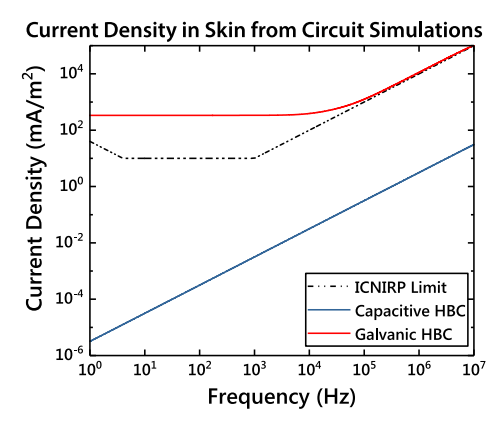


Fig. 3. Current density in the skin adjacent to the device, calculated from circuit model.

field, different physical quantities are used to set the restriction of exposure. For frequencies in 1 Hz-10 MHz range, current density provides the restriction to prevent effects on central nervous system. In the 100 MHz-10 GHz range restrictions are provided on Specific energy Absorption Rate (SAR) to prevent heat stress on the body. Between the 10 GHz–300 GHz frequency range, power density is restricted to prevent heating in body tissue or near the skin surface. The limits on these restrictions are shown in graphical form in Fig. 3. As can be seen from the plots, the most stringent requirement on *current density* is in the 4 Hz-1 KHz frequency range due to the low threshold current required for nerve stimulation at this frequency range. In addition to the whole body SAR requirement of 0.08 W/Kg, the restriction of localized SAR in head and trunk is 2 W/Kg and limbs are 4 W/Kg. Apart from these, reference level for time varying contact current, when the human body comes in contact with an object of different electrical potential, are provided in order to avoid shock and burn hazards. For frequency of <2.5 KHz the maximum contact current is 0.5 mA, whereas for 2.5-100 KHz the limit is 0.2 f (f = frequency in KHz) and for >100 KHz the limit is 20 mA.

# B. Institute of Electrical and Electronics Engineers (IEEE) Standard

The IEEE standard also provides guidelines for Basic Restrictions (BR) and Maximum Possible Exposure (MPE) limits of the human body to time varying electric, magnetic fields and contact currents in the 3kHz to 300 GHz frequency range. Separate restriction limits are provided for sinusoidal and pulsed electric fields and contact currents, as well as for fields and signals with multiple frequency components. Most of this limits show close correspondence to the ICNIRP guidelines discussed in the previous subsection. The standard also looks into multiple previous studies which has explored different cancer and non-cancer related effects of these radiations. It looks into studies which takes care of the established thermal effects of RF frequencies above 100 kHz and electrostimulation effect below 100 kHz. A review of non-cancer studies about the effect of these fields on thermoregulation, neurochemistry, neuropathology teratogenicity, reproduction, development, auditory pathology, membrane biochemistry is provided with most of them showing minimal or no effects. Cancer related studies on DNA damage, cell cycle elongation, cell toxicity, gene and protein expression and activity also does not show any clear or consistent role of RF radiation on human cancer. It also provides recommendations such as usage of bi-phasic signal to avoid harmful electro-chemical action on the electrode, skin interface.

# C. The National Institute for Occupational Safety and Health (NIOSH) Standard

While the previous two standards primarily looks into the effect of current density and field intensities of lower values on the human body, the NIOSH standards looks into the effect of high voltage and current on the human body. Electric current chooses the path of least resistance within the body, and dissipates heat during the passage, which can cause thermal damage to tissue along the path of current. The skin provides the highest resistance to flow of current. Skin resistance, when dry, is about 300 times greater than the resistance of internal organs. This high resistance of skin is lowered in several ways: by cuts and abrasions, by immersion in water, by breakdown of outer layer of skin by high voltages >600 Volts, thereby allowing large amount of current to pass and cause greater damage. The tissues that sustain highest damage from electrical injury are nerve, muscle, bone and skin. Nerves sustain direct damage from the passage of electricity, with proprioceptive nerves being the most susceptible. The passage of current can also overstimulate the nervous system, and cause varying degrees of damage to internal organs.

The physiological effect of electric injury is determined by the magnitude of the current passing through the human body. Higher voltage generally causes greater acute injury to the human body, however, the reverse can be true as well. High-voltage ( $\sim$ 103 Volts) arcing can often throw the victim off by blast effect,

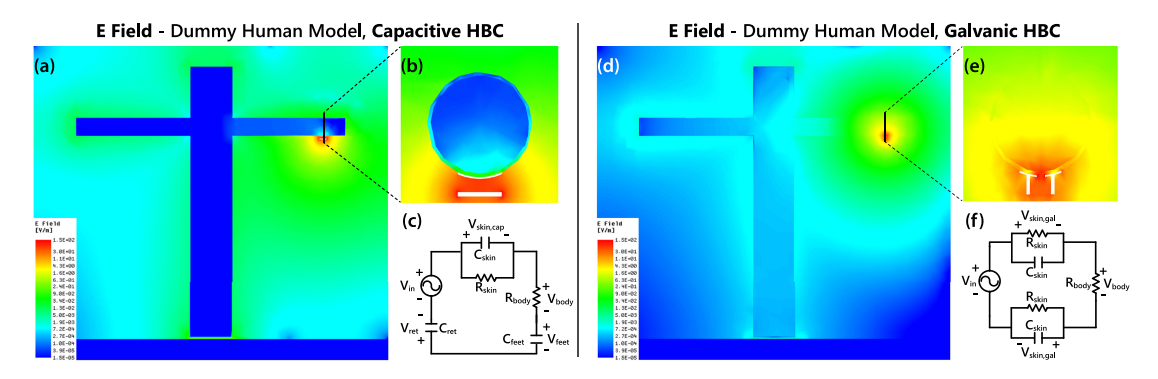


Fig. 4. **Capacitive HBC:** Electric field distribution along (a) a cross-section plane of the dummy model of Fig. 5 and (b) a cross-section of the arm and the device as shown in Fig. 5b, (c) simplified channel model. **Galvanic HBC:** Electric field distributions (d) across the body and (e) near the device, (f) simplified channel model. All simulations for these field distributions were carried out at 400 kHz, for a 1 V p-p sinusoidal excitation voltage.

thereby limiting contact and hence extent of injury; whereas a much lower voltage 60-Hz AC current can cause an involuntary muscle contraction with protracted gripping, prolonging contact and leading to far more severe injury. The outcome of electrical injuries, whatever the mode of causation, is heavily dependent on the speed of initiation of initial resuscitative measures.

There have been a few previous studies exploring the safety aspect of HBC. [27] explores the safety aspect of galvanic HBC. In this paper, the authors use empirical arm models to find the safe operable range of galvanic HBC, subject to field intensity and Specific Absorption Rate (SAR) restrictions. The authors of [28] uses COMSOL to build a 3D numerical arm model and solve equations to get the current densities at 3 different frequencies (100 kHz, 1 MHz, 10 MHz) for different body conditions (wet skin/dry skin) and excitation electrode areas. The authors conclude that for low frequency operation at 100 kHz the current density exceeds the safety limits. The authors in [29] analyses the thermal distribution in tissues through numerical methods for galvanic HBC by varying the amount of power transmitted and the number of co-located transmitters and conclude that the temperature increase due to galvanic HBC stays way below the safety limit of 1 °C.

In the subsequent sections we will carry out circuit and FEM based simulations to compare the induced current and field densities with the safety limit established by the standards discussed in this section.

#### IV. THEORETICAL SAFETY ANALYSIS

We carry out theoretical studies through circuit and FEM modeling and simulations to analyze the safety compliance of HBC in terms of current and field constraints respectively. This section looks into the setup for both these analysis and provide a quantitative measure of safety.

## A. Bio-Physical Model of HBC

We use an experimentally validated Bio-Physical model [1] of the human body to find a reasonable estimate of the current and field densities within the body and analyze the safety aspect. The model consists of different human body biological parameters

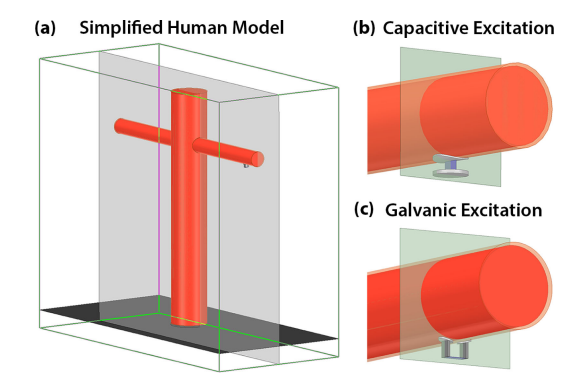


Fig. 5. (a) Dummy human model consisting of two crossed cylinders with muscle interior and 4mm thick skin shell. The cross-section plane shown is used for E field plots in Fig. 4a and Fig. 4d. (b) Excitation structure for capacitive HBC. A potential difference is maintained between a copper disc of 2 cm radius attached to skin and a floating copper ground plate. The cross-section plane is for E field plot in Fig. 4b. (c) Excitation structure for galvanic HBC. A potential difference is maintained between two copper discs of 1 cm radius, placed 2 cm apart on the skin. The cross-section plane is for E field plot in Fig. 4e.

along with the different parasitic capacitance for capacitive HBC. The load conditions are also included in the circuit models, although they do not play a critical role in determining the current density or field intensity within the body, The details of the Bio-Physical model along with the component values in a tabular form can be found in [1] and is provided in Fig. 2. In this paper we use a relatively simplified version of the complete Bio-Physical model, consisting of the components required to explain the field distribution and current density within the body.

## B. Current Density Limits: Circuit Simulation

Theoretical simulations are carried out for both capacitive and galvanic HBC to find the current density within the body resulting from voltage excitation provided to the skin. A Bio-Physical model [1] of the human body is used for simulation purposes. An AC analysis of the circuit provides us with the current being injected into the body across different frequencies. This is then compared with the safety limit provided by the guidelines.

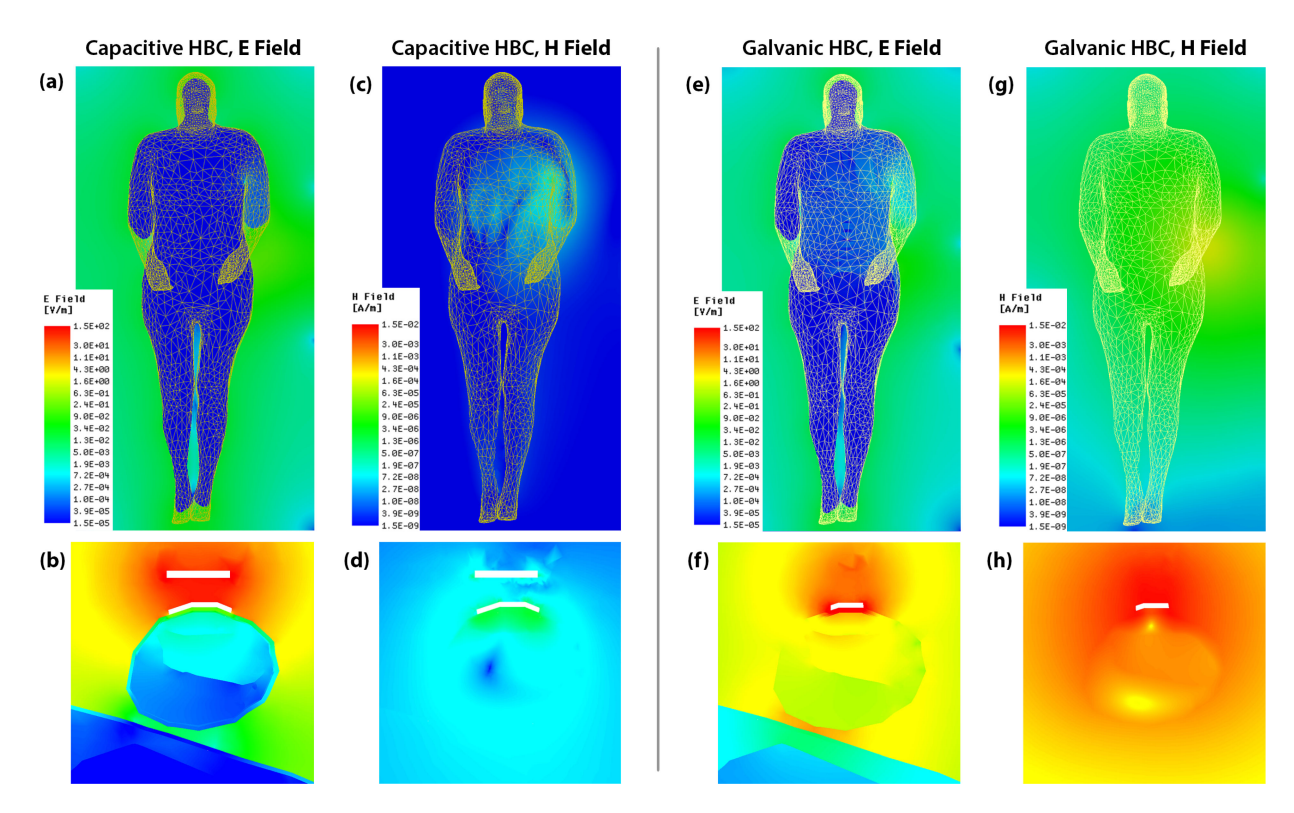


Fig. 6. Field plots along different cross section planes of the detailed human model shown in Fig. 7 at 400 kHz, 1 V p-p sinusoidal excitation voltage. **Capacitive HBC:** (a) E field across the body, (b) E field near the device, (c) H field across the body, and (d) H field near the device. **Galvanic HBC:** (e) E field across the body, (f) E field near the device, (g) H field across the body, and (h) H field near the device.

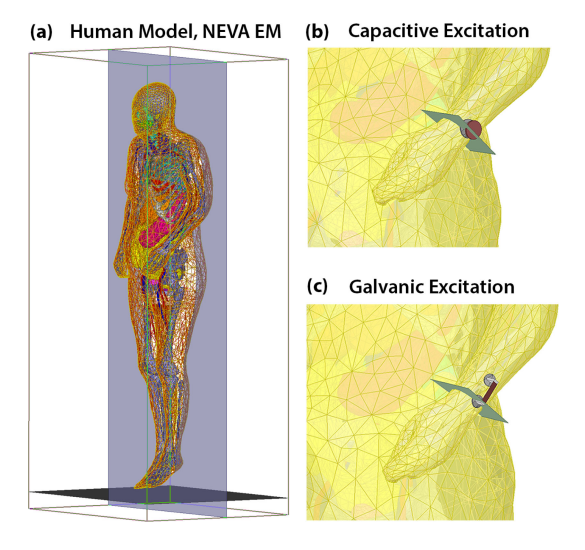


Fig. 7. (a) Detailed human model for FEM simulations: VHP-Female v2.2 from NEVA Electromagnetics LLC, with cross-section plane for E and H field plots of Fig. 6a, 6c, 6e and 6g. (b) excitation method for capacitive HBC and cross section plane for obtaining field plots of Fig. 6b and 6d, and (c) excitation method for galvanic HBC and cross section plane for obtaining field plots of Fig. 6f and 6h.

As seen from the detailed Bio-Physical model in Fig. 2 and the simplified versions in Fig. 4c, f, the return path in capacitive HBC is closed by the parasitic capacitances between the ground plane of the transmitter, receiver devices and the surrounding environment. The impedance of this parasitic capacitance is the

primary limitation in the amount of current flowing through the body for capacitive HBC. The value of this capacitance is in the order of a few picofarads, Hence, the impedance provided by the return path is few  $M\Omega$  for frequencies less than the MHz range. This limits the current to a few  $\mu A$  for capacitive HBC, The maximum current density will be close to the electrodes used for excitation. Taking a cross sectional area equal to the size of the electrode (4 cm²) close to it, the current density is plotted across different frequency, as shown in Fig. 3, for an excitation voltage of 1 V. It can be seen that the current density is orders of magnitude smaller than the safety limits suggested by the ICNIRP guidelines for the general public. This shows that capacitive HBC complies with the safety limit.

In case of galvanic HBC, the signal is applied differentially between two electrodes, both connected to the body. Hence there is a closed loop formed between the signal and ground terminal (Fig. 4f), through the body. The skin provides the impedance between the signal and the ground electrode and is in the order of few tens of  $K\Omega$ . Hence, the amount of current injected into the body is significantly higher compared to capacitive HBC. As shown in Fig. 4e, most of the current is primarily contained within the surface of the skin. Hence, the cross sectional area of the current transmission is taken considering the thickness of the skin (4 mm maximum). The plot of current density is shown in Fig. 3, for an excitation voltage of 1 V applied through excitation at the wrist with a distance of 2 cm between the electrodes. This shows that applying signals to the wrist, as done in several previous studies, can result in localized current densities, which

is significantly higher than the recommended general public safety limit, at the skin close to the signal electrode. To ensure safety compliance in case of galvanic HBC, a *current limiting circuit* can be used at the output of HBC devices to ensure that the current injected into the body is within the recommended safety limits for general public exposure.

## C. Field Limits: FEM Simulations

To understand the E and H field distributions in and around the human body for both capacitive and galvanic HBC, simulations were performed in Ansys High-Frequency Structure Simulator (HFSS), which is an FEM based EM solver. First, simulations are carried out using a simplified model consisting of two crossed cylinders as shown in Fig. 5 to develop an idea of the expected field distributions for both capacitive and galvanic HBC. The dielectric properties of this model is assigned as that of an average human muscle, and it is given a 4mm thick skin shell. Dielectric and conductive properties of human body tissues found by Gabriel et al. [30] is used for all EM simulations in this section. The simplified model enables us to explain the field distribution intuitively from the voltage drop obtained through circuit models and provide a connection between the field and circuit simulations; this will later be backed by detailed full-body simulations derived from the model shown in Fig. 7. For capacitive HBC, the excitation is provided by a single disc shaped conductor attached to the skin, and an alternating potential difference is maintained between this and another disc shaped plate hanging in the air that is supposed to serve as the ground plate of the device (Fig. 5b). As shown in the simplified circuit representation of this modality in Fig. 4c, derived from Fig. 2, the signal return path from the subjects body to the device ground plate is formed via parasitic capacitance to earth ground. The impedance of this capacitance is high compared to the resistance provided by human muscle, and the potential drop inside the subjects body should be negligible. This in turn implies that the electric field inside the body should be low, which is confirmed from the E Field plots from the simulation (Fig. 4a and Fig. 4b). For galvanic HBC, the excitation is provided by two disc shaped conductors placed 2 cm apart on the skin (Fig. 5c), and an alternating potential difference is maintained between the two. This results into a high potential difference at the skin over a short distance, resulting into a high local electric field inside the subjects body, especially at the skin (Fig. 4e). For both capacitive and galvanic styles of excitation, a voltage source is used in HFSS. A voltage source is preferred over a lumped port style excitation, because the results from a lumped port has possibilities of getting affected by port impedance and reflections at the excitation point depending on the model design, whereas a voltage source in HFSS basically represents an ideal voltage source, maintaining an alternating potential difference of 1 V between the points of excitation, no mater what the design is. This provides us with a more fundamental platform to study field and current patterns in HBC.

This basic simulation setup is now carried over to a detailed model of human body, to find out values of E and H fields that different body parts would experience for a certain HBC

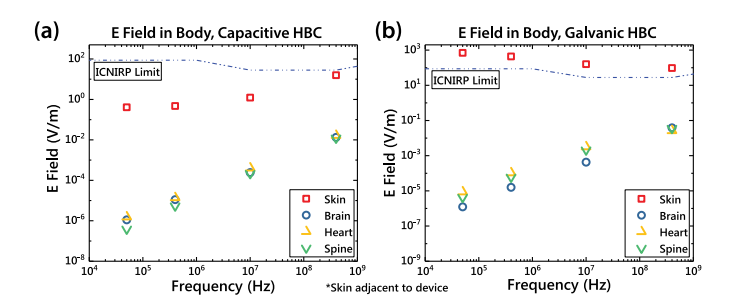


Fig. 8. Maximum RMS E fields at different parts of the body from simulations of the detailed human model of Fig. 7 with 1 V p-p sinusoidal excitation for (a) capacitive HBC, and (b) galvanic HBC. For galvanic HBC, the fields at the skin adjacent to the device is above the ICNIRP limit.

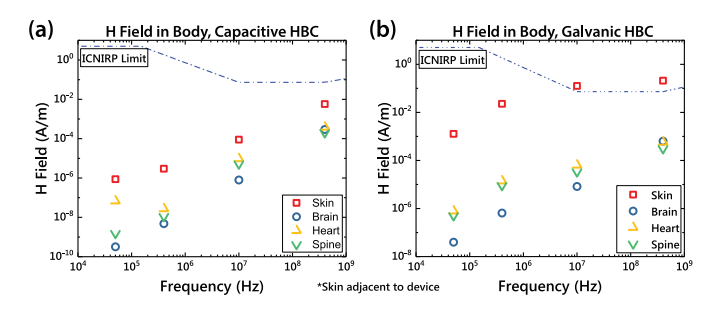


Fig. 9. Maximum RMS H fields at different parts of the body from simulations of the detailed human model of Fig. 7 with 1 V p-p sinusoidal excitation for (a) capacitive HBC, and (b) galvanic HBC. For galvanic HBC, the fields at the skin adjacent to the device is above the ICNIRP limit at frequencies over 10 MHz.

operating voltage. The human body model used for all the simulations was obtained from NEVA Electromagnetics LLC. The specific model used is the VHP-Female v2.2, which was generated from a 162 cm tall, 60 year old female subject [31]. The HFSS simulation setup used is shown in Fig. 7. Similar to the simulations of the cylindrical dummy model, the excitations were provided by a single disc and a floating ground plate in capacitive HBC (Fig. 7b), and two spaced disc in case of galvanic HBC (Fig. 7c). As mentioned before, the dielectric properties of the body tissues were adapted from the works of Gabriel et al. [30]; we did not use the material properties that came packaged with the HFSS version of the NEVA EM model, as the HFSS model did not incorporate tissue properties for frequencies less than 10 MHz. The field plots resulting from simulations of the detailed model shown in Fig. 6 suggest the same key points noted in the simulations of the dummy, i.e. lower fields inside the body for capacitive HBC compared to galvanic, and high local fields near the device, notably in the skin, for galvanic HBC. Simulations were performed for multiple frequencies in the 100 kHz-1 GHz range, and maximum RMS E and H field values were recorded at the skin patch below the device, as well as a few vital organs such as brain, heart and the spinal cord. The comparison of these values with the ICNIRP limit for general public exposure is shown in Fig. 8 and Fig. 9. It is evident that for 1 V excitation, the fields at brain, heart or spinal cord remain well below the ICNIRP threshold for both capacitive and galvanic HBC. Additionally for capacitive HBC, the fields at the skin adjacent to the HBC device are below the safety limit as well, whereas these local fields ride above the threshold for galvanic HBC with fixed potential and without any current limiting circuit at the output of the transmitter. This indicates the need for current limiting circuits at the output of HBC transmitters to ensure compliance of current density and field limits under all usage scenarios.

#### D. Field Estimation From Circuit Model

The Bio-Physical circuit models of capacitive (Fig. 4c) and galvanic HBC (Fig. 4f) provides an intuitive explanation to the expected electric field and explains which mode of operation creates higher fields. As seen from the EM simulations, the field density is highest near the skin where the signal is injected. The voltage drop across the skin determines the electric field density ( $E = \frac{V}{d}$ ). From the Bio-Physical model of capacitive HBC (Fig. 4) the voltage drop across skin and the field density can be obtained as in equation (1) and (3) respectively.

$$V_{skin,cap} = \frac{V_{in} * Z_{skin}}{Z_{skin} + \frac{1}{sC_{ret}} + \frac{1}{sC_{fret}} + R_{body}}$$
(1)

$$Z_{skin} = R_{skin} \parallel \frac{1}{sC_{skin}} \tag{2}$$

$$E_{skin,cap} = \frac{V_{skin,cap}}{t_{skin}} \tag{3}$$

The impedance of the skin is in the range of 10 s of  $K\Omega$ , varying with body conditions. The return path capacitance is dominated by the self-capacitance of the device and is around a few pFs [1], [32]. Only when the transmitter comes in very close proximity of the ground plane (few cms) the distance between the device and the external ground has an effect on the return path capacitance . Hence, for all practical purposes, the return path capacitance is almost independent of the distance of the transmitter from the ground. Since the return path impedance is significantly larger than the skin impedance for frequencies up to 10 s of MHz range, the voltage drop across the skin is significantly small. As a result, the generated field is also small across the skin, whose thickness is presented as 4 mm.

The Bio-Physical model for galvanic HBC (Fig. 4f) shows that the impedance across the transmitter is primarily dependent on the skin impedance. The impedance provided by the internal tissue layers are in the order of few 100 s of  $\Omega$  s and smaller than the skin impedance (10 s of K  $\Omega$ ). Hence, for galvanic HBC, the voltage drop across the skin (eq. (4)) is a significant portion of the applied voltage. So, the electric field density across the skin (eq. (5)) for galvanic HBC is significantly higher compared to capacitive HBC. This can be validated from the field plots obtained through HFSS simulations in Fig. 4a and Fig. 4b.

$$V_{skin,gal} = \frac{V_{in} * Z_{skin}}{2Z_{skin} + R_{body}} \tag{4}$$

$$E_{skin,gal} = \frac{V_{skin,gal}}{t_{chin}} \tag{5}$$

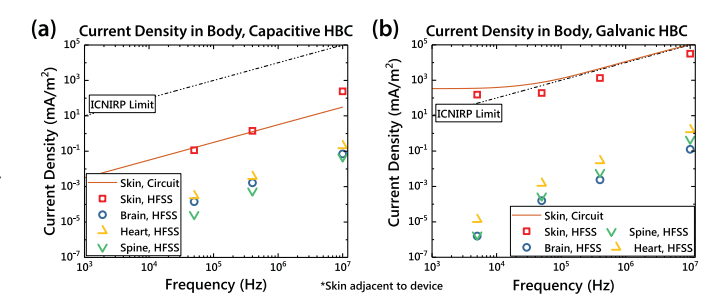


Fig. 10. RMS current densities at different parts of the body from simulations of the detailed human model of Fig. 7 with 1 V p-p sinusoidal excitation for (a) capacitive HBC, and (b) galvanic HBC. The current density at the skin adjacent to the device is also computed using a circuit theoretic model, and all values are compared with the ICNIRP limit for general public exposure.

### E. Current Density Limits: FEM Simulations

Similar to the electric and magnetic field limits, the current density within the body can also be estimated from the HFSS simulations. Fig. 10 shows the current density on different parts of the body for a 1 V p-p sinusoidal excitation for capacitive (Fig. 10a) and galvanic HBC (Fig. 10b). The current density limits for capacitive HBC is significantly smaller than the safety limits imposed by the guidelines. In case of galvanic HBC though, the current density on the skin near the excitation point is close to the safety limits. The current density results on the skin obtained from circuit simulations of the bio-physical model is also shown in Fig. 10 and corroborates the safety of capacitive HBC in terms of current density.

## V. SAFETY ANALYSIS: EXPERIMENTS

The previous sections establishes the safety of capacitive HBC from theory, both in terms of current density and electric/magnetic field intensity, through circuit and FEM simulations. The results show order of magnitude difference between the safety limits and the simulated current density, fields compared to the safety limits. To further corroborate and support the safety of HBC, we collect the vital parameters of human subjects and carry out a statistical analysis and provide experimental evidence that HBC does not show any early signs of affecting the vital parameters of subjects.

## A. Experimental Design and Methods

1) Study Design: To ascertain the existence of any short-term effect of HBC on the human body, a study was designed to non-invasively measure a set of commonly used five vital parameters from human subjects both in and without the presence of HBC devices. The study was approved by the Institute Review Board (IRB). Seven subjects took part in the experiments through voluntary consent. The vital parameters observed are the Heart Rate (HR), Blood Pressure (BP), Respiratory Rate (RR), oxygen saturation of hemoglobin (SpO<sub>2</sub>) and body temperature (Temp) of the test subject.

2) Experimental Procedure: The volunteers were first monitored for their baseline vital parameters for a day. On the following three days the volunteers were the HBC enabled

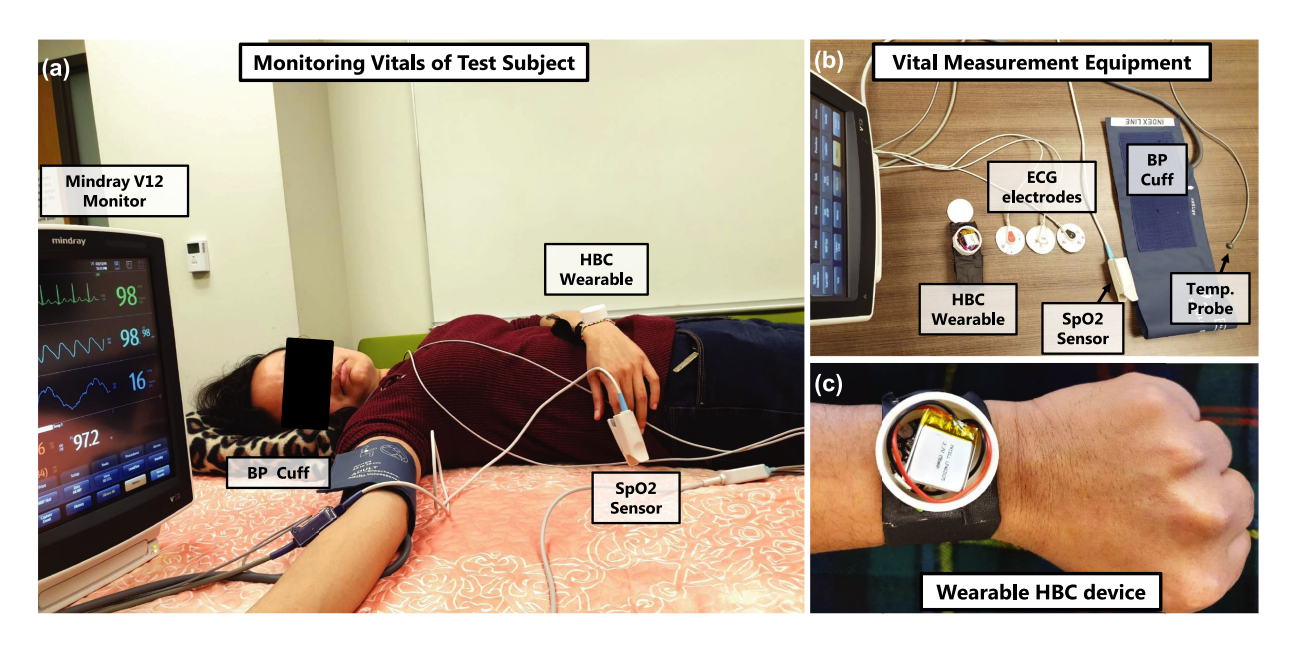


Fig. 11. Diagram showing the experimental setup for measuring the vital parameters of human subjects. (a) Vital recordings carried out on a test subject, wearing a HBC transmitter device, using the Mindray V12 patient monitor, (b) Details showing the equipment used for different measurements with the patient monitor, (c) The HBC wearable device showing on the wrist of a test subject.

watch-like wearable (Fig. 11c), during which their vital parameters were recorded for three time slots on each day. Following the set of measurements with the HBC device on, more baseline measurements are carried out for the vital parameters. The time slot distribution for these experiments are shown in Fig. 12b. These set of measurements were carried out multiple times almost over a month.

- *3) Equipment and Facilities:* A medical grade patient monitor (MindRay V12), was used for measuring the vitals. The sensors used are ECG probes and gel electrodes, SpO<sub>2</sub> sensor, BP cuff and Temperature probe sourced from Mindray. The study design, preparation of subjects, experimental data collection and results of data analysis were supervised by a medical doctor.
- 4) HBC Device Design: The wearable 'watch-like' HBC device (Fig. 11c) consists of a microcontoller, a LiPo battery, a custom-made stretchable band with a copper electrode on the underside of the band touching the human skin, all housed in a small 3D printed round housing for easy all-day wearability for the volunteers. The device consists of a 32-bit Cortex M0+ ATSAMD21E18 microcontroller, which is programmed to digitally synthesize the electrical excitation at 400 KHz with 3.3 V peak to peak amplitude. This signal is then coupled into the body through a 2 cm  $\times$  2 cm copper electrode. For all our experiments we carry out measurements for capacitive HBC, as this is our preferred mode of HBC, based on the theoretical analysis presented above. A single electrode is used to excite the signal into the body and the ground electrode remains floating. The HBC device is worn on the wrist of the volunteer.
- 5) Data Collection and Statistical Analysis: To ascertain the effects of HBC compared to a normal scenario, baseline data of the vital parameters of these subjects were also recorded on separate days, before and after they had put on the HBC

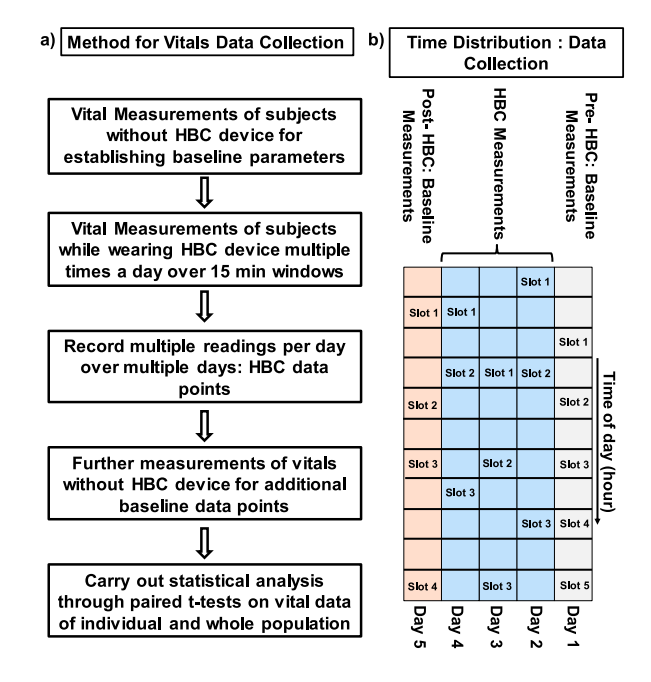


Fig. 12. (a) Flow graph showing the method of vital data collection on test subjects. Measurements are first carried out to establish the baseline for each subject. Multiple following measurements were carried out with the HBC device worn by the test subjects on multiple days. Further baseline measurements are done following the completion of the tests with the HBC wearable device. (b) Time slot distribution showing the type of data collected (baseline vs HBC data) over the different days of experiment.

enabled wearable. The goal of the experiments is to observe whether wearing the HBC enabled device has an effect on the vital parameters of the person through statistical analysis. Fig. 11 shows the details of the experimental setup. Fig. 11a

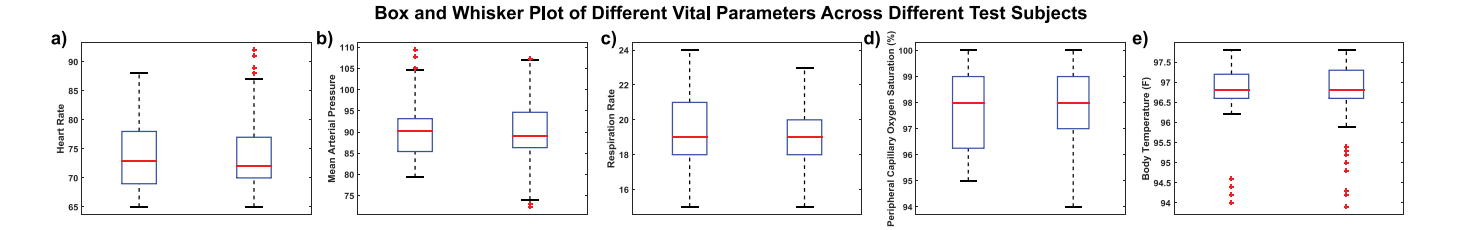


Fig. 13. Box and Whisker plot for the different vital parameters of the human subjects with and without wearing the HBC enabled device: (a) Heart Rate (HR), (b) Mean Arterial Pressure (MAP), (c) Respiration Rate (RR), (d) Peripheral Capillary Oxygen Saturation (SpO<sub>2</sub>), (e) Body Temperature. There is minimal change in the mean value and ranges of the vital parameters across the entire population in presence of signal transmission through HBC, compared to a normal scenario, showing HBC does not affect the vitals of the body.

shows the vital monitoring being carried out on one of the volunteers with a Mindray V12 patient monitor. The details of the different sensors used for the vital measurements are shown in Fig. 11b.

Each recording was made as a set of 5 data points. At the start of each recording, the monitor is connected to the human subject to record the vital information. Three gel electrode leads were placed, one each at the two arms and one at the left leg, and the tracing was chosen similar to that of a standard ECG Lead II. BP was measured by means of an adult-sized BP cuff on the right arm that was set to inflate at intervals of 5 mins. The temperature probe was placed in contact with skin in the left axillary region. SpO<sub>2</sub> was measured by the pulse oximeter placed to clasp the tip of the left index finger. After the connection were made and the volunteers vitals attained steady-state, four consecutive readings were taken off the monitor display, concurrent with the 5-minute inflation interval of the BP cuff. Each data collection session lasted about 15 mins. Multiple such sessions of recordings were made throughout the day on each volunteer over five days. The data recordings were done on 7 human subjects (4 male, 3 female) aged in the twenties and early thirties. a flow graph showing the complete data collection procedure is shown in Fig. 12a.

For each vital parameter, baseline readings were pooled together, and readings with HBC device on were pooled together. The range and 95% confidence interval of each subject was constructed from the data, both in the baseline state and Intra-HBC state, for each vital parameter. This allowed us to look for any significant change due to HBC in each individual subject. The Two-Sample t-test was used for this purpose. The p-values are also calculated to understand the statistical significance of the change in parameters, if any, as a result of wearing an HBC enabled device.

#### B. Results

The statistical analysis is done through Paired t-test of baseline data and the data with HBC wearable on, for each vital parameter. We carry out the t-test on both the individual and population vitals data. Individual t-tests are run to gather more statistical information, which can be limited from the population tests due to the relatively small population size. Hence, baseline and HBC measurements are carried out on individual test subjects multiple number of times to have sufficient statistical significance.

TABLE I
P VALUES FOR T TESTS OF INDIVIDUAL SUBJECTS

	Gender	HR	MAP	RR	$SpO_2$	Temp
S1	Male	0.16	0.26	0.55	0.18	0.31
S2	Male	0.28	0.56	0.41	0.19	0.09
S3	Male	0.11	0.98	0.21	0.50	0.57
S4	Female	0.34	0.40	0.49	0.29	0.39
S5	Female	0.79	0.06	0.52	0.28	0.58
S6	Male	0.27	0.45	0.60	0.48	0.40
S7	Female	0.39	0.06	0.68	0.59	0.70

TABLE II
MEAN DIFFERENCE FOR T TESTS OF INDIVIDUAL SUBJECTS

	Gender	HR	MAP	RR	$SpO_2$	Temp
S1	Male	1.98	0.91	0.31	0.57	0.12
S2	Male	2.00	0.71	0.77	0.59	0.22
S3	Male	1.01	0.03	0.74	0.28	0.06
S4	Female	1.24	0.65	0.48	0.36	0.09
S5	Female	0.56	2.02	0.47	0.47	0.22
S6	Male	2.02	1.12	0.42	0.29	0.06
S7	Female	0.76	1.46	0.18	0.11	0.03
S7	Female	0.76	1.46	0.18	0.11	0.03

The p values obtained from individual t-test results are shown in Table I. It can be seen that the p values for all vital parameters for each individual is >0.05, indicating that HBC does not introduce any significant statistical change in the vital parameters of the subjects. The mean values of the vital parameters also show minimal change between the baseline scenario and with the HBC device on the test subject as shown in Table II. Fig. 14 shows the box and whisker plot for the HR, MAP, SpO<sub>2</sub> and temperature measurements of two individual test subjects, showing small difference in the mean values and the ranges. Similarly the population box and whisker plots (Fig. 13) for all the different vital parameters show that there is little change in the mean and range of the parameters between the states when the subject is wearing the HBC enabled device and when he/she is not wearing it.

For looking at the changes in parameter in the entire population, the Paired t-test was used with the two variables being the Baseline mean and the Intra-HBC mean for each of the 7 subjects. Five such paired t-tests were done for the five vital parameters under consideration. The p values and the mean differences obtained from these tests also does not show any statistically significant change.

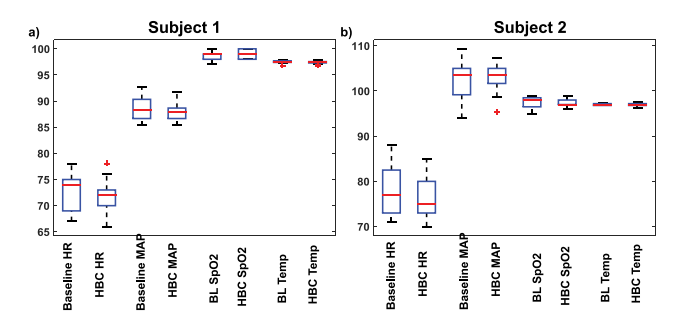


Fig. 14. Box and Whisker plot of HR, MAP, SpO<sub>2</sub>, Body Temperature of two test subjects. Similar to the population ranges, the individual plots also do not show any significant change in the mean value and ranges of the vitals. Subject 1 is a male subject and subject 2 is female.

## VI. DISCUSSIONS

The different safety standards reviewed in this paper shows that the restriction limitations come from the limit on current density, Specific Absorption Rate and maximum field exposure. Certain design practices can be adopted to ensure safety compliance of the HBC devices even under varying conditions of the human body when nominal conditions are not satisfied. For example, the impedance provided by the human body can vary significantly (by orders of magnitude) in presence of sweat or a wound in the skin. This can lead to varying amount of current flowing through the body depending on the physical condition, which can lead to currents exceeding the safety limit being injected into the body. From circuit design point of view any HBC device can be designed with a current limiter circuit at the output to ensure the injected current into the body is within the safety limits even under varying physiological condition. Such design practices need to be followed while designing HBC circuits and systems to ensure compliance with the safety limits at all frequencies and different mode of operation of the device.

### VII. CONCLUSION

HBC is a promising alternative to wireless radio wave based communication of devices around the body, due to its enhanced security and energy efficiency. However, the safety aspect of HBC needs to be carefully evaluated as it involves injecting electrical current into the body, This paper, for the first time, provides a thorough analysis of the safety compliance of different types of HBC by FEM, circuit simulations and carries out a small experimental study to observe any effect of HBC on the vital parameters of the human body. The simulations show that the current density and field intensities in capacitive HBC are significantly smaller compared to the safety standards. Statistical analysis of the vital parameters of human subjects involved in the experimental study show statistically insignificant change due to wearing a HBC device, supporting the simulation results. On the other hand, galvanic HBC with differential excitation at the wrist can result in localized current densities and field intensities (around the electrode), which are significantly higher than the safety limits and should be avoided. This small non-clinical study didn't show any early sign of the effect of HBC on the vitals of the subjects and the simulations showed large margin of

safety. In future longer clinical studies can be done before HBC is adopted as a widely used product. Future studies about the safety aspect of HBC can employ invasive procedures on a wider population to see the effect of electrical signals on extracellular fluids, nerves, muscles and neuromuscular junctions.

#### **ACKNOWLEDGMENT**

The authors would like to thank Mr. Shitij Avlani for his help in designing the HBC wearable device.

#### **REFERENCES**

- [1] S. Maity *et al.*, "Biophysical modeling, characterization and optimization of electro-quasistatic human body communication," *IEEE Trans. Biomed. Eng.*, vol. 66, no. 6, pp. 1791–1802, Jun. 2019.
- [2] S. Maity et al., "A 6.3 pj/b 30 mbps -30 dB SIR-tolerant broadband interference-robust human body communication transceiver using time domain signal-interference separation," in *Proc. IEEE Custom Integr. Circuits Conf.*, Apr. 2018, pp. 1–4.
- [3] S. Maity, D. Das, and S. Sen, "Wearable health monitoring using capacitive voltage-mode human body communication," in *Proc. 39th Annu. Int. Conf. IEEE Eng. Medicine Biol. Soc.*, Jul. 2017, pp. 1–4.
- [4] J. Park and P. P. Mercier, "Magnetic human body communication," in *Proc.* 37th Annu. Int. Conf. IEEE Eng. Med. Biol. Soc., Aug. 2015, pp. 1841– 1844.
- [5] Z. Lucev, I. Krois, and M. Cifrek, "A capacitive intrabody communication channel from 100 kHz to 100 MHz," in *Proc. IEEE Int. Instrum. Meas. Technol. Conf.*, May 2011, pp. 1–4.
- [6] J. Park, H. Garudadri, and P. P. Mercier, "Channel modeling of miniaturized battery-powered capacitive human body communication systems," *IEEE Trans. Biomed. Eng.*, vol. 64, no. 2, pp. 452–462, Feb. 2017.
- [7] N. Cho et al., "The human body characteristics as a signal transmission medium for intrabody communication," *IEEE Trans. Microw. Theory Techn.*, vol. 55, no. 5, pp. 1080–1086, May 2007.
- [8] Y. Song, Q. Hao, and K. Zhang, "Review of the modeling, simulation and implement of intra-body communication," *Defence Technol.*, vol. 9, no. 1, pp. 10–17, Mar. 2013. [Online]. Available: http://www.sciencedirect.com/ science/article/pii/S2214914713000238
- [9] S. Maity et al., "Characterization of human body forward path loss and variability effects in voltage-mode HBC," *IEEE Microw. Wireless Com*ponents Lett., vol. 28, no. 3, pp. 266–268, Mar. 2018.
- [10] H. Cho et al., "21.1 A 79 pj/b 80 mb/s full-duplex transceiver and a 42.5 W 100 kb/s super-regenerative transceiver for body channel communication," in Proc. IEEE Int. Solid-State Circuits Conf. Dig. Tech. Papers, Feb. 2015, pp. 1–3.
- [11] H. Cho, J. Bae, and H. J. Yoo, "A 39 μw body channel communication wake-up receiver with injection-locking ring-oscillator for wireless body area network," in *Proc. IEEE Int. Symp. Circuits Syst.*, May 2012, pp. 2641–2644
- [12] N. Cho et al., "A 60 kb/s-10 Mb/s adaptive frequency hopping transceiver for interference-resilient body channel communication," *IEEE J. Solid-State Circuits*, vol. 44, no. 3, pp. 708–717, Mar. 2009.
- [13] M. A. Callejn et al., "A comprehensive study into intrabody communication measurements," *IEEE Trans. Instrum. Meas.*, vol. 62, no. 9, pp. 2446–2455, Sep. 2013.
- [14] S. Maity et al., "Secure Human-Internet using dynamic human body communication," in Proc. IEEE/ACM Int. Symp. Low Power Electron. Des., Jul. 2017, pp. 1–6.
- [15] B. Chatterjee et al., "Context-aware intelligence in resource-constrained iot nodes: Opportunities and challenges," *IEEE Des. Test*, vol. 36, no. 2, pp. 7–40, Apr. 2019.
- [16] S. Sen, "Invited: Context-aware energy-efficient communication for IoT sensor nodes," in *Proc. 53nd ACM/EDAC/IEEE Design Automat. Conf.* (DAC), Austin, TX, USA, 2016, pp. 1–6.
- [17] S. Maity, D. Das, and S. Sen, "Adaptive interference rejection in human body communication using variable duty cycle integrating DDR receiver," in *Proc. Des., Autom. Test Eur. Conf. Exhib.*, Mar. 2017, pp. 1763–1768.
- [18] S. Maity *et al.*, "BodyWire: A 6.3-pJ/b 30-Mb/s -30-dB SIR-tolerant broadband interference-robust human body communication transceiver using time domain interference rejection," *IEEE J. Solid-State Circuits*, vol. 54, no. 10, pp. 2892–2906, Oct. 2019.

- [19] S. Maity et al., "A 415 nW physically and mathematically secure electroquasistatic HBC node in 65 nm CMOS for authentication and medical applications," in Proc. IEEE Custom Integr. Circuits Conf. (CICC), Boston, MA, USA, 2020, pp. 1–4.
- [20] M. Hessar, V. Iyer, and S. Gollakota, "Enabling on-body transmissions with commodity devices," in *Proc. ACM Int. Joint Conf. Pervasive Ubiquitous Comput.*, 2016, pp. 1100–1111. [Online]. Available: http://doi.acm. org/10.1145/2971648.2971682
- [21] D. Das et al., "Enabling covert body area network using electroquasistatic human body communication," Sci. Rep., vol. 9, no. q, pp. 19:1– 19:36, Mar. 2019. [Online]. Available: https://doi.org/10.1038/s41598-018-38303-x
- [22] M. Kono et al., "Design guideline for developing safe systems that apply electricity to the human body," ACM Trans. Comput.-Hum. Interact., vol. 25, no. 3, pp. 19:1–19:36, Jun. 2018. [Online]. Available: http://doi.acm.org/10.1145/3184743
- [23] T. G. Zimmerman, "Personal Area Networks: Near-field intrabody communication," *IBM Syst. J.*, vol. 35, no. 3.4, pp. 609–617, 1996.
- [24] M. S. Wegmueller *et al.*, "Signal transmission by galvanic coupling through the human body," *IEEE Trans. Instrum. Meas.*, vol. 59, no. 4, pp. 963–969, Apr. 2010.
- [25] S. Maity et al., "Characterization and classification of human body channel as a function of excitation and termination modalities," in Proc. 40th Annu. Int. Conf. IEEE Eng. Medicine Biol. Soc. (EMBC), Honolulu, HI, USA, 2018, pp. 3754–3757.

- [26] ICNIRP, "ICNIRP guidelines for limiting exposure to timevarying electric and magnetic fields (1 Hz–100 KHz)," *Health Phys.*, vol. 99, no. 6, pp. 818–836, 2010.
- [27] Y.-M. Gao et al., "Electrical exposure analysis of galvanic-coupled intrabody communication based on the empirical arm models," BioMedical Eng. OnLine, vol. 17, no. 71, 2018. [Online]. Available: https://doi.org/ 10.1186/s12938-018-0473-9
- [28] Ž. Lučev, A. Koričan, and M. Cifrek, "A finite element method study of the current density distribution in a capacitive intrabody communication system," in XII Mediterranean Conf. Medical and Biological Eng. Comput., P. D. Bamidis and N. Pallikarakis, Eds. Berlin, Germany: Springer, 2010, pp. 422–425.
- [29] M. Swaminathan, U. Muncuk, and K. R. Chowdhury, "Tissue safety analysis and duty cycle planning for galvanic coupled intra-body communication," in *Proc. IEEE Int. Conf. Commun.*, May 2016, pp. 1–6.
- [30] S. Gabriel, R. W. Lau, and C. Gabriel, "The dielectric properties of biological tissues: II. measurements in the frequency range 10 hz to 20 GHz," *Phys. Med. Biol.*, vol. 41, no. 11, pp. 2251–2269, Nov. 1996.
  [31] S. N. Makarov *et al.*, "Virtual human models for electromagnetic studies
- [31] S. N. Makarov et al., "Virtual human models for electromagnetic studies and their applications," *IEEE Rev. Biomed. Eng.*, vol. 10, pp. 95–121, 2017.
- [32] M. Nath, S. Maity, and S. Sen, "Towards understanding the return path capacitance in capacitive human body communication," *IEEE Trans. Cir*cuits Syst. II: Express Briefs, vol. 67, no. 10, pp. 1879–1883, Oct. 2020.